

Effect of Atmospheric Turbulence on Acquisition Time of Ground to Deep Space Optical Communication System

Hemani Kaushal, V.K.Jain, and Subrat Kar

Abstract—The performance of ground to deep space optical communication systems is degraded by distortion of the beam as it propagates through the turbulent atmosphere. Turbulence causes fluctuations in the intensity of the received signal which ultimately affects the acquisition time required to acquire and locate the space-borne target using narrow laser beam. In this paper, performance of free-space optical (FSO) communication system in atmospheric turbulence has been analyzed in terms of acquisition time for coherent and non-coherent modulation schemes. Numerical results presented in graphical and tabular forms show that the acquisition time increases with the increase in turbulence level. This is true for both schemes. The BPSK has lowest acquisition time among all schemes. In non-coherent schemes, M -PPM performs better than the other schemes. With the increase in M , acquisition time becomes lower, but at the cost of increase in system complexity.

Keywords—Atmospheric Turbulence, Acquisition Time, Binary Phase Shift Keying (BPSK), Free-Space Optical (FSO) Communication System, M -ary Pulse Position Modulation (M -PPM), Coherent/Non-coherent Modulation Schemes.

I. INTRODUCTION

IN recent years, free-space optical (FSO) communication systems have received growing attention owing to its unique features: extremely high bandwidth, rapid deployment time, tariff-free bandwidth allocation, low power consumption, weight and size. However, when optical beam propagates through the atmosphere, it experiences fluctuations in amplitude and phase due to atmospheric turbulence. These intensity and phase fluctuations cause the beam to wander and pose challenges for the ground based station to acquire and locate the space-borne receivers normally defined within a certain uncertainty region. The effect of atmospheric turbulence is different for different modulation schemes and hence acquisition time required to cover an uncertainty solid angle will be different. Acquisition process requires a laser beam to cover an uncertainty solid angle and to detect that beam at the receiving end. There are several techniques to accomplish this initial uncertainty solid angle coverage [1]. Most commonly used is the stare/scan technique. It involves staring the receiver viewfield and scanning a narrow beam laser over an uncertainty area. By using narrow beam divergence laser, sufficient power is available to enable signal detection. Hence stare/scan technique is used to evaluate acquisition time in atmospheric turbulent environment.

H. Kaushal, S. Kar are with the Department of Electrical Engineering, Indian Institute of Technology, Delhi, Hauz Khas, New Delhi 110016, India (email: himaniz@yahoo.com, subrat@ee.iitd.ac.in).

V.K.Jain is with the Dept. of Electr. & Electronics Engn., Universiti Teknologi PETRONAS (UTP), Malaysia (drvirander_jain@petronas.com.my).

This paper is organized as follows: The model of the atmospheric channel under weak and strong turbulent conditions is described in Section II. Configuration of acquisition link to determine the uncertainty area is discussed in Section III. The performance of coherent and non-coherent modulation schemes in atmospheric turbulence is analyzed in Section IV. Numerical results in graphical and tabular forms are presented in section V. Finally, in Section VI, conclusions of the analysis are given.

II. LIGHT WAVE PROPAGATION IN ATMOSPHERIC TURBULENCE

The atmospheric channel is one of the most complex channels in the communication world. This channel may change its characteristics by more than two orders of magnitude per kilometer, depending on weather conditions [2]. There are two major challenges encountered in FSO systems. First, owing to the narrow beam width, active pointing, acquisition and tracking (PAT) mechanism is required to combat the effect of beam wandering, beam steering etc. Second is the need to combat link fading due to scattering and scintillation. Amongst these, the major impairment of FSO system comes from the atmospheric induced scintillation. The main source of scintillation is the random fluctuations in the index of refraction due to the inhomogeneities in temperature and pressure of the atmosphere along the transmission path. This phenomenon is known as atmospheric turbulence [3, 4].

In the following section, models for atmospheric turbulence and fading distribution of light wave signal are given.

A. Atmospheric Turbulence Model

When a laser beam propagates through the atmosphere, it can experience random phase and amplitude fluctuations due to atmospheric turbulence. Turbulence effects on the propagation of laser beam arise from the refractive index fluctuations due to temperature gradients induced in the atmosphere by solar heating. Hence turbulent eddies can be visualized as being fixed in the atmosphere and moving with the wind. This model is usually referred to as the 'frozen-in' model of turbulence.

Atmospheric turbulence can be physically described by Kolmogorov theory [5]. A widely used model with good accuracy was proposed by Kolmogorov, which assumes the wavenumber spectrum to be

$$\Phi_n(\vec{k}) = 0.033 C_n^2 k^{-11/3} \quad (1)$$

where C_n^2 is the structure parameter of refractive index, which is altitude dependent and k is given by $(2\pi/l)$ where l is eddy scale size. It is the most important parameter to characterize the laser beam disturbance caused by refractive

index fluctuations. For ground to deep space communication, Hufnagel-Valley model of C_n^2 is widely used and is given by [6]

$$C_n^2 = 2.72 \times 10^{-16} \left[3V^2 \left(\frac{h}{10} \right)^{10} \exp(-h) + \exp\left(\frac{-h}{1.5}\right) \right] \quad (\text{m}^{-2/3}) \quad (2)$$

where V is the root mean square value of the wind speed in m/s which influences the high altitude turbulence and h altitude in km.

The atmospheric turbulence leads to fluctuations in the log-amplitude X of the received signal. Based on the atmosphere turbulence model, analytic expression for the variance of log-amplitude fluctuations can be obtained and is given by [6]

$$\sigma_\lambda^2 = 4.78 (\sec \theta)^{11/6} \lambda^{-7/6} \int_0^L C_n^2(z) (z')^{5/6} dz \quad (3)$$

where $z' = z$ for downlink and $z' = L - z$ for uplink. L is the height of space-borne receiver (uplink) or transmitter (downlink). For receiver altitude well above the turbulent atmosphere, this integral becomes independent of altitude. Substitution of Eqn. (2) in Eqn. (3) yields variance of log-amplitude fluctuations as

$$\sigma_\lambda^2 = \left[7.41 \times 10^{-2} \left(\frac{V}{27} \right)^2 + 4.45 \times 10^{-3} \right] \lambda^{-7/6} (\sec \theta)^{11/6} \quad (4)$$

where θ is the zenith angle and λ the operating wavelength in μm . Fig. 1 shows the plot of Eqn. (4) for $\lambda = 1.55 \mu\text{m}$ as a function of V for various values of θ .

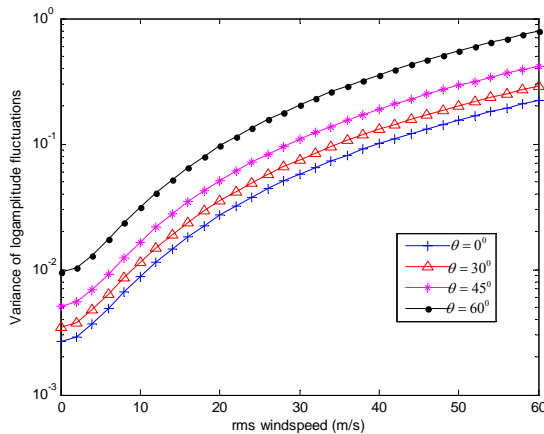


Fig. 1 Variance of log-amplitude fluctuations σ_λ^2 as a function of rms wind speed V for different θ

B. Probability Distribution of Fading Light Wave Intensity

Based upon the atmospheric turbulence theory mentioned above, it has been seen that atmospheric turbulence leads to fluctuations in log-amplitude X . The statistical properties of log-amplitude fluctuations also referred as intensity fading, is derived in this section. Several models exist to study the statistical properties of the intensity fluctuations under varying atmospheric conditions, though none is accepted universally, since atmospheric conditions are unpredictable.

In case of weak turbulence, the central-limit theorem gives the marginal distribution of log-amplitude X as Gaussian which is given as

$$f_x(X) = \frac{1}{\sqrt{2\pi\sigma_\lambda^2}} \exp \left\{ -\frac{(X - E[X])^2}{2\sigma_\lambda^2} \right\} \quad (5)$$

The received signal intensity I is related to log-amplitude X by

$$I = I_0 \exp(2X - E[X]) \quad (6)$$

where I_0 is the average signal light intensity without turbulence and $E[X]$ is the ensemble average of log-amplitude X . From Eqs.(5) and (6), the average light intensity is

$$E[I] = E[I_0 \exp(2X - E[X])] = I_0 \exp(2\sigma_\lambda^2) \quad (7)$$

Hence the marginal distribution of light intensity fading induced by weak turbulence is log-normal as below [7].

$$f_I(I) = \frac{1}{2I\sqrt{2\pi\sigma_\lambda^2}} \exp \left\{ -\frac{[\ln(I) - \ln(I_0)]^2}{8\sigma_\lambda^2} \right\} \quad (8)$$

In case of strong turbulence, the central-limit theorem gives a complex Gaussian field whose amplitude is Rayleigh distributed. Hence, the marginal distribution of light intensity fading induced by strong turbulence is given by a negative exponential model [8].

$$f_I(I) = \frac{1}{I_0} \exp \left(-\frac{I}{I_0} \right) \quad (9)$$

The range of validity of log-normal and negative exponential models is usually expressed in terms of normalized intensity variance also called scintillation index (σ_{SI}^2) defined as [9]

$$\sigma_{SI}^2 = \frac{E[I^2]}{E[I]^2} - 1 \quad (10)$$

The pdf in Eqn. (8) remains valid for σ_{SI} in the range of [0, 0.75]. In case of strong turbulence, $\sigma_{SI} = 1$ (or in the vicinity of 1). This index is related to variance of log-amplitude fluctuations σ_λ^2 as $\sigma_{SI}^2 = \exp(\sigma_\lambda^2) - 1$ [10]. It can also be written as

$$\sigma_\lambda^2 = \ln(\sigma_{SI}^2 + 1) \quad (11)$$

For a given value of σ_{SI}^2 , one can compute variance of log-amplitude fluctuations.

III. CONFIGURING THE ACQUISITION LINK

Acquisition requires searching the uncertainty area to locate and establish a link between ground station and distant space-borne target. The basic contributors to the initial uncertainty are shown in Fig. 2. Considering all the contributors, uncertainty area of 5 mrad has been considered in this paper.

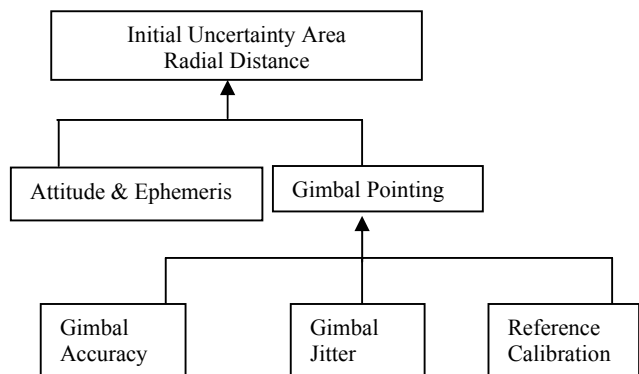


Fig. 2 Initial uncertainty contributors from ground to space-borne targets

A. Acquisition Time and Beam Divergence

For acquisition, we have chosen a transmitter scan and receiver stare mode of operation. The acquisition time is given by

$$t_{acq} = \left[\frac{\theta_{unc}^2}{\theta_{beam}^2 \times \xi_t} \right] \times T_{dwell} \times N_t \quad (12)$$

where θ_{unc} is the uncertainty area diameter, θ_{beam} the beam divergence of transmit laser source exciting the aperture, T_{dwell} the time transmitter dwells in any location and N_t the number of total transmitter scan area repeats. The parameter, ξ_t is the overlap factor that acquisition designer add to the beam to provide some additional margin of safety against large high frequency jitter fluctuations.

The acquisition is a two step process. First, there must be sufficient signal for initial detection and second, a sufficient received energy to allow closed loop tracking to begin. Thus the bound on beam divergence comes from the required acquisition time and transition power margin. The choice of beam divergence is thus very critical to provide enough received signal energy to support the initial detection of target in required acquisition time and transition to narrow beam tracking. The received signal energy per pulse is given by

$$E_r = \frac{E_t \times D_r^2}{\theta_{beam}^2 \times (R)^2} \quad (13)$$

where E_t is the emitted energy per pulse, D_r the diameter of receiver aperture and R the range of about 40,000 kms. Further, the required signal for acquisition link depends upon the detection criteria. In this paper, phase locked loop (PLL) technique is considered to provide sufficient loop SNR. The lock time (i.e., the time to detect) drives the scan time in the acquisition process and ultimately the time to acquire the acquisition process. It is given by

$$T_{lock} = \frac{4.2(\Delta f)^2}{B_{loop}^3} \quad (14)$$

where Δf is the frequency offset of PLL. For a loop lock time of 5 ms and frequency offset of 10% of acquisition tone frequency (10 kHz), the required loop bandwidth is 943.5 Hz.

B. Acquisition Noise Density

The noise density for acquisition is determined from the preamplifier noise, the detector dark noise and the background noise. The background noise energy is restricted by the use of narrowband filters. The source spectral width limits the passband width of the filter. The field of view (FOV) is restricted by the spot size. In this paper, background noise is determined using 5 mrad FOV.

The background noise power for the lunar disk on axis is given as [11]

$$P_B = H_B \cdot \left(\frac{\pi}{4} \right) (FOV)^2 B_f \cdot \left(\frac{\pi}{4} \right) (D_r)^2 L_R \quad (15)$$

where H_B is the background radiant flux, B_f the bandwidth of optical rejection filter in angstrom and L_R the optical losses in the receiver system.

With noise power as in Eqn. (15), background noise current density for an APD detector is given as

$$i_b^2 = 2qFR_0P_B \text{ (A}^2\text{/Hz)} \quad (16)$$

where q is the electron charge, F the excess noise factor of APD, R_0 the detector responsivity. For 5 mrad FOV and 60 Å

Vol:3, No:2, 2009 and pass filter, responsivity of 0.87 $\mu\text{A}/\mu\text{W}$ and excess noise factor of 3.18 are chosen.

The detector dark current is given by

$$i_d^2 = 2qR_0FP_{dm} + 2qR_0P_{du} \text{ (A}^2\text{/Hz)} \quad (17)$$

where P_{dm} and P_{du} are the total multiplied and total unmultiplied power, respectively. Also preamplifier noise current density is given as

$$i_{pa}^2 = \frac{(NEI)^2}{M^2} \text{ (A}^2\text{/Hz)} \quad (18)$$

where NEI is the preamplifier noise equivalent current, M the APD gain. In this paper NEI of approximately $2.1 \times 10^{-12} \text{ A} / \sqrt{\text{Hz}}$ and $M=150$ are taken. Also, for acquisition of coherent system local oscillator noise is given by

$$i_{lo}^2 = 2qR_0FP_{lo} \text{ (A}^2\text{/Hz)} \quad (19)$$

The total noise for coherent system and non-coherent system, respectively are given by

$$\sigma_{tot-acq}^2 = \sigma_b^2 + \sigma_d^2 + \sigma_{pa}^2 + \sigma_{lo}^2 \text{ (A}^2\text{/Hz)} \quad (20)$$

and

$$\sigma_{tot-acq}^2 = \sigma_b^2 + \sigma_d^2 + \sigma_{pa}^2 \text{ (A}^2\text{/Hz)} \quad (21)$$

IV. PERFORMANCE ANALYSIS IN ATMOSPHERIC TURBULENCE

The received signal energy helps to determine the acquisition time for the space-borne receivers. But the received energy at the detector is affected by atmospheric turbulence. Further, effect of turbulence on the performance of coherent and non-coherent modulation schemes is different. Error probability analyses of both these schemes in weak as well as strong atmospheric turbulence have been carried out in this section.

The bit error probability without turbulence is given by

$$P_e = Q(\sqrt{SNR}) \quad (22)$$

where $Q(\cdot)$ is the Gaussian Q -function defined as

$$Q(x) = \frac{1}{2\sqrt{\pi}} \int_x^\infty \exp^{-y^2/2} dy \quad (23)$$

$$= \frac{1}{\pi} \int_0^{\pi/2} \exp\left(-\frac{x^2}{2\sin^2\theta}\right) d\theta \quad (24)$$

In the presence of turbulence, conditioning on the fading coefficient gives

$$P_e = Q(\sqrt{SNR(I)}) \quad (25)$$

Averaging over the fading coefficient, we obtain

$$P_e = \int_0^\infty f_I(I) Q(\sqrt{SNR(I)}) dI \quad (26)$$

In case of weak turbulence $f_I(I)$ is given by Eqn. (8) and for strong turbulence by Eqn. (9). The signal-to-noise ratio (SNR) without turbulence is given by [12]

$$SNR = \frac{\sigma_s^2}{\sigma_n^2} = \frac{I^2}{FI + I_n} \quad (27)$$

In the above equation, I_n is the average noise intensity in the received signal.

A. Performance Evaluation of Coherent and Non-Coherent Modulation Schemes

Following the approach mentioned above, performance of coherent schemes (BPSK and QPSK) and non-coherent schemes (OOK and M-PPM) are analyzed in both weak and strong turbulence scenario and the results are given in Figs.3 and 4 and Tables I and II.

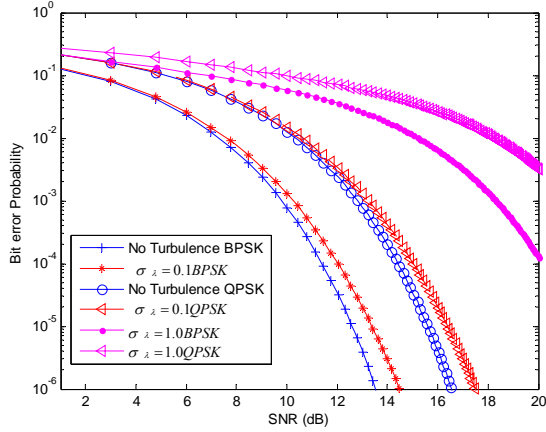


Fig. 3 Error performance of BPSK and QPSK for weak turbulence $\sigma_\lambda = 0.1$ and strong turbulence $\sigma_\lambda = 1.0$

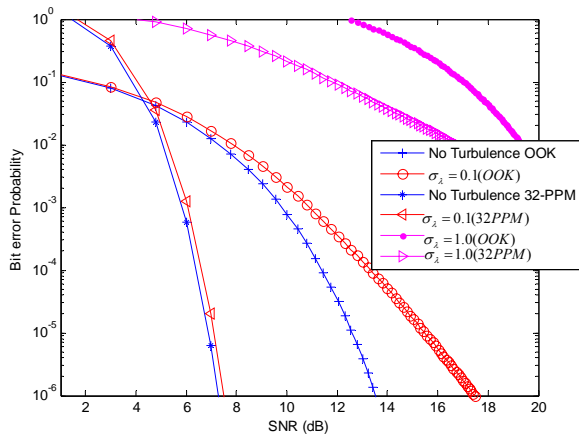


Fig. 4 Error performance of OOK and 32-PPM for weak turbulence $\sigma_\lambda = 0.1$ and strong turbulence $\sigma_\lambda = 1.0$

For the computation, first of all the required received signal power is calculated for a BER of 10^{-3} . Then using Eqn. (13), beam divergence is calculated for a given receiver diameter ranging from 15 cm to 30 cm for the space-borne receiver [13]. Finally acquisition time is evaluated using Eqn.(12) for uncertainty area of 5 mrad, dwell time of 10 ms and total of 60 scan area repeats. In the computation, ξ_t is taken to be 0.15. Further, all calculations are made for transmitted average

power level of 500 mW. Variations of acquisition time with receiver diameter operating at 1550 nm wavelength under weak ($\sigma_\lambda = 0.1$) and strong ($\sigma_\lambda = 1.0$) turbulence condition at BER of 10^{-3} for coherent and non-coherent schemes are shown in Figs. 5 and 6 and Tables I and II.

V. RESULTS AND DISCUSSION

It is observed from Figs. 3-6 and Tables I and II that the BPSK modulation scheme gives lower acquisition time in weak as well as strong turbulence than the other modulation schemes. Among non-coherent schemes, M-PPM gives better performance than OOK system. It may be mentioned that trend of error curve remains the same for an error rate of 10^{-6} .

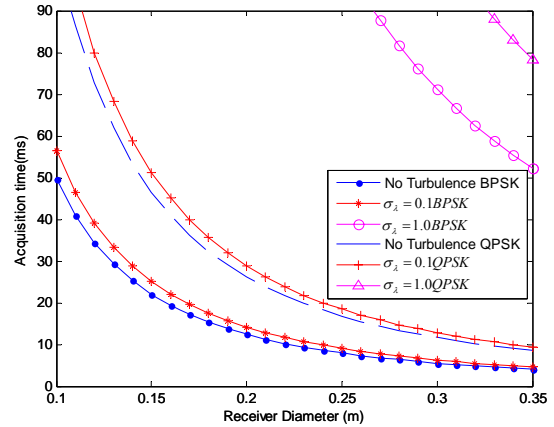


Fig.5 Acquisition time of coherent modulation schemes in weak turbulence $\sigma_\lambda = 0.1$ and strong turbulence $\sigma_\lambda = 1.0$

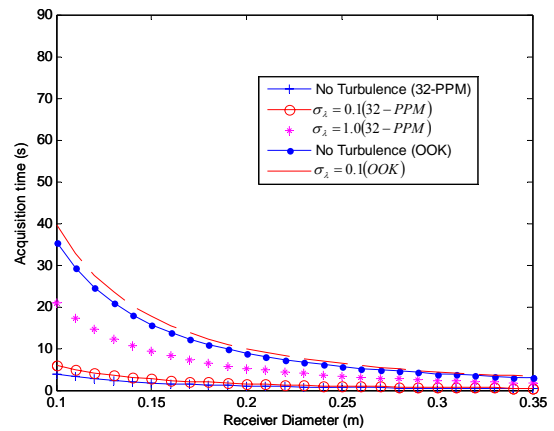


Fig. 6 Acquisition time of non-coherent modulation schemes in weak turbulence $\sigma_\lambda = 0.1$ and strong turbulence $\sigma_\lambda = 1.0$

Modulation schemes	Measuring quantity	No Turbulence	$\sigma_i=0.1$	$\sigma_i=0.2$	$\sigma_i=0.3$	$\sigma_i=0.5$	$\sigma_i=0.7$
BPSK	Rq power(W)	1.55×10^{-15}	1.76×10^{-15}	2.41×10^{-15}	3.61×10^{-15}	1.10×10^{-14}	1.60×10^{-14}
	Acq time(ms)	5.5	6.2	8.5	12.8	38.3	57.27
QPSK	Rq power(W)	3.27×10^{-15}	3.61×10^{-15}	4.80×10^{-15}	7.21×10^{-15}	2.19×10^{-14}	2.32×10^{-14}
	Acq time(ms)	11.7	12.8	17.1	25.6	77.86	82.48
OOK	Rq power(W)	1.11×10^{-12}	1.24×10^{-12}	2.89×10^{-12}	*	*	*
	Acq time(ms)	3946	4400	10300	*	*	*
2-PPM	Rq power(W)	9.63×10^{-13}	1.18×10^{-12}	1.36×10^{-12}	1.57×10^{-12}	1.97×10^{-12}	2.42×10^{-12}
	Acq time(ms)	3424	4195	4835	5582	7004	8604
32-PPM	Rq power(W)	1.21×10^{-13}	1.59×10^{-13}	1.94×10^{-13}	2.30×10^{-13}	3.04×10^{-13}	3.4×10^{-13}
	Acq time(ms)	430	565	689	817	1080	1208
256-PPM	Rq power(W)	3.48×10^{-14}	4.92×10^{-14}	6.27×10^{-14}	7.59×10^{-14}	1.07×10^{-13}	1.42×10^{-13}
	Acq time(ms)	124	174	222	269	380	504

“*” Implies that BER=10⁻³ is not achievable and therefore it is not possible to achieve acquisition.

TABLE II

ACQUISITION TIME FOR 30 CM RECEIVER DIAMETER FOR COHERENT AND NON-COHERENT MODULATION SCHEMES OPERATING AT 1550 NM IN STRONG TURBULENCE FOR BER=10⁻³

Modulation schemes	Measuring quantity	BER=10 ⁻⁶	BER=10 ⁻³
BPSK	Rq power(W)	*	2.23×10^{-14}
	Acq time(ms)	*	77
QPSK	Rq power(W)	*	3.62×10^{-14}
	Acq time(ms)	*	128
OOK	Rq power(W)	*	*
	Acq time(ms)	*	*
2-PPM	Rq power(W)	7.41×10^{-12}	4.55×10^{-12}
	Acq time(ms)	26346	16177
32-PPM	Rq power(W)	9.29×10^{-13}	6.53×10^{-13}
	Acq time(ms)	3303	2321
256-PPM	Rq power(W)	2.78×10^{-13}	2.08×10^{-13}
	Acq time(ms)	988	739

“*” Implies that the required BER is not achievable

A correlation between received power level and acquisition time is seen from Tables I and II. That is lower the required power, lesser will be the acquisition time. Since BPSK and QPSK are coherent schemes; they have increased sensitivity and can detect a lower level of power. With this low power level, acquisition time becomes less as observed from the tables. In contrast to this, non-coherent schemes require higher power levels and, therefore, will have more acquisition time. This is the price one need to pay in addition to decreased sensitivity for non-coherent schemes.

VI. CONCLUSION

Performance of coherent and non-coherent systems has been analyzed in terms acquisition time under zero, weak and strong turbulence. The acquisition time increases with increase in the turbulence level. This is true for both coherent and non-coherent modulation schemes. The BPSK has lowest acquisition time among coherent and non-coherent modulation schemes. In non-coherent schemes, *M*-PPM performs better than the other schemes. Higher is the value of *M*, lesser is the acquisition time, but more is the system complexity.

REFERENCES

- [1] Van Hove and Chan, "Optical satellite networks," Journal of Lightwave Technology. vol. 21, no. 11, pp. 2811, Nov 2003.
- [2] H. Manor and S. Arnon, "Performance of an optical wireless communication system as a function of wavelength," Applied Optics. vol. 42, no. 21, pp. 4285-4294, 2003.
- [3] J.Strohbehn, Ed., "Laser Beam Propagation in the Atmosphere", New York: Springer, 1978.
- [4] V.Tatarski, "Wave Propagation in Turbulent Medium," New York: McGraw-Hill, 1961.
- [5] D.L.Fried, "Scintillation of a ground to space laser illuminator," Journal of Optical Society of America, vol. 57, no.8, pp. 980-983, 1967.
- [6] H.T.Yura and W.G.McKinley, "Optical scintillation statistics for IR ground to space laser communication systems," Applied Optics, vol. 22, no. 21, pp. 3353-3358, Nov 1983.
- [7] X.Zhu and J.M.Kahn, "Free-space optical communication through atmospheric turbulence channels," IEEE Transactions on Communications, vol.50, no.8, pp.1293-1300, August 2002.
- [8] Jagtar Singh and V.K.Jain, "Performance analysis of BPPM and M-ary PPM optical communication systems in atmospheric turbulence," IETE Technical Review, vol. 25, no. 4, pp.146-156, 2008.
- [9] S. Karp, R. M. Gagliardi, S. E. Moran and L. B. Stotts, "Optical Channels," New York, Plenum press, 1988.
- [10] Kamran Kiasaleh, "Performance of APD-based, PPM free-space optical communication systems in atmospheric turbulence," IEEE Transactions on Communications, vol. 53, no. 9, pp.1455-1461, 2005.
- [11] Stephen G.Lambert and William L.Casey, "Laser Communication in Space," Artech House, London, 1995.
- [12] S.Karp and R.M.Gagliardi, "Optical Communication," 2nd Edition, John Wiley, 1995.
- [13] Alexander H.Hemmati, S.Monacos, et al., "System requirement for a deep space optical transceivers," JPL, California Institute of Technology, Pasadena, May 2005.